Journal of Pediatric Surgery 56 (2021) 352–359

Contents lists available at ScienceDirect

Journal of Pediatric Surgery

journal homepage: www.elsevier.com/locate/jpedsurg

Deletion of interleukin enhancer binding factor 2 (ILF2) resulted in defective biliary development and bile flow blockage

Yim Cheung [a], Zhongluan Wu [a], Maria-Mercedes Garcia-Barcelo [a,b], Paul Kwong Hang Tam [a,b,c], Alvin Chung Hang Ma [d], Vincent Chi Hang Lui [a,b,c,*]

[a] Department of Surgery, LKS Faculty of Medicine, The University of Hong Kong, Hong Kong, 21 Sassoon Road, Pokfulam, Hong Kong
[b] Dr. Li Dak-Sum Research Centre, The University of Hong Kong–Karolinska Institutet Collaboration in Regenerative Medicine, 5/F The Hong Kong Jockey Club Building for Interdisciplinary Research, The University of Hong Kong 5 Sassoon Road, Pokfulam, Hong Kong
[c] Department of Surgery, The University of Hong Kong–Shenzhen Hospital, 1, Haiyuan 1st Road, Futian District, Shenzhen, Guangdong, P.R.C.
[d] Department of Health Technology and Informatics, The Hong Kong Polytechnic University, Hong Kong, 9/F, Lee Shau Kee Building, The Hong Kong Polytechnic University, Hung Hom, Kowloon, Hong Kong

ARTICLE INFO

Article history:
Received 3 March 2020
Received in revised form 29 May 2020
Accepted 18 June 2020

Key words:
Liver
Bile duct
Biliary atresia
ILF2
Zebrafish

ABSTRACT

Purpose: Biliary atresia (BA) is a devastating obstructive bile duct disease of newborns. BA has the highest incidence in Asians (1/5000), and its pathogenesis is unclear. We identified BA-private rare copy number variants (CNVs; 22 duplications and 6 deletions). *ILF2* gene locates in the chromosome region (Chr1:153410347–153,634,058) which was deleted in a nonsyndromic BA patient. However, it is still not known whether *ILF2* plays a role in hepatobiliary development and its deletion impacts on the bile duct development.
Methods: To investigate if *ILF2* is required for biliary development, we knock-out the zebrafish homologs of *ILF2* by CRISPR/Cas9 approach, and discover that deletion of ILF2 causes a defective biliary development and a lack of bile flow from the liver to the gall bladder in zebrafish, which is a resemblance of phenotypes of BA.
Results: Our data indicate that *ILF2* gene is required for biliary development; deletion of *ILF2* impairs bile duct development and could contribute to BA pathogenesis. This will be the first study to functionally evaluate the genes interfered by BA-private CNVs in hepatobiliary development and in BA pathogenesis.
Conclusions: Such functional study may reveal the potential value of these BA-private CNVs in the disease pathogenesis for BA.
Level of evidence: N/A (animal and laboratory study).

Biliary atresia (BA [OMIM 210500]) is a devastating inflammatory cholangiopathy affecting 5–14:100,000 live births and is a predominant cause for prolonged neonatal jaundice [1–3]. Without surgery (Kasai procedure) to reestablish the bile drainage, patients develop liver failure and die by the age of two [3,4]. However, postsurgical complications, including cholangitis (bile duct infection) (50% of patients) and portal hypertension (>60% of patients), remain a problem [4]. Furthermore, regardless of drainage after surgery, patients will often develop bile duct inflammation and sclerosis, leading to secondary biliary cirrhosis [5–8]. Liver transplantation is the only option for those patients developing secondary biliary cirrhosis and those who failed surgery.

BA can be classified into two groups according to the origin of the etiopathogenic process: a) syndromic form (5%–10% of the cases in Caucasians, <3% in Asians), which is attributed to defective morphogenesis of the bile-duct during development and present mostly syndromic; and b) nonsyndromic form (>90% of cases), in which bile-ducts undergo obliteration in the perinatal period. The pathogenesis of BA is still unknown. It is now believed that most forms of the BA may start before birth, and any factors that induce biliary damage in utero should be considered as etiological factors [9].

Genomic rearrangements leading to the appearance of copy number variations (CNVs). CNVs are frequent and widespread events, cause our phenotypic diversity and play an important role in human disease. By various molecular mechanisms, including gene dosage, gene disruption, gene fusion, and position effects, CNVs can cause Mendelian or sporadic traits, or be associated with complex diseases. To assess the genotype–phenotype correlation between rare copy number variants (CNVs) and BA, we called CNVs from our GWAS [10,11] and identified 28 BA-

* Corresponding author at: Department of Surgery, LKS Faculty of Medicine, The University of Hong Kong, Hong Kong, 21 Sassoon Road, Pokfulam, Hong Kong. Tel: +852 39179607; fax: +852 39179621.
E-mail address: vchlui@hku.hk (V.C.H. Lui).

https://doi.org/10.1016/j.jpedsurg.2020.06.032

unique CNV regions (>100 kb each; 6 deletions and 22 duplications) that interfered with a total of 102 genes (76 duplicated and 26 deleted). These BA-CNVs biologically converged into immune pathway, suggesting that genes relevant in immune regulation within BA-CNVs likely contributed to BA [12]. The current theory is that developmental errors that occur somewhere along the differentiation/morphogenesis of the biliary tree during embryonic period lead to defective hepatobiliary system, upon exposure to an unknown environmental factor during the perinatal period, which induces an uncontrollable and potentially self-limiting immune response from the innate immune system, manifested as liver fibrosis and atresia of the hepatic bile ducts of BA.

ILF2 gene was first identified to encode a 45 kDa transcription factor namely interleukin enhancer binding factor 2 (ILF2; also known as NF45), which is required for T-cell expression of the interleukin 2 gene, and involved in immune-regulation [13–15]. However, ILF2 is also involved in diverse cellular processes and functions in many different cell types. By forming a complex with the interleukin enhancer-binding factor 3 (NF90, ILF3), ILF2 affects the cytoplasmic distribution and stability [16,17], processing and translation [18–20] of mRNA, repairs DNA breaks [21,22], and negatively regulates the microRNA processing [23]. Furthermore, ILF2/ILF3 complex also regulates cell cycle exit and myogenic differentiation [24,25], pluripotency and differentiation of embryonic stem cells [26]. However, there is no literature on the roles of *ILF2* in hepatobiliary development and its relevance in experimental or clinical BA. In this study, *ILF2* was chosen for functional evaluation in biliary development because of its expression in human liver [27], its diverse functions in the pluripotency, proliferation and lineage differentiation of stem cells [24–26], and it locates in the chromosome region (Chr1:153410347–153,634,058) which is deleted in a nonsyndromic BA patient [12].

To investigate if *ILF2* is required for biliary development, we knockout the zebrafish homologs of *ILF2* by CRISPR/Cas9 approach, and discover that deletion of *ILF2* causes a defective biliary development and a lack of bile flow from the liver to the gall bladder in zebrafish, which is a resemblance of phenotypes of BA.

1. Methods

1.1. Zebrafish

Wild-type zebrafish and transgenic zebrafish (*Danio rerio*) lines (um14Tg[Tg(tp1-MmHbb:EGFP)um14] (ZL1950) were purchased from Zebrafish International Resource Center ((ZIRC), 5274 University of Oregon, Eugene, OR 97403-5274, USA). [(um14Tg[Tg(tp1-MmHbb:EGFP)um14] transgenic fish expressed strong green fluorescent protein signal in both the intra- and extrahepatic bile ducts [28–31]. Zebrafish embryos were obtained from natural spawning. Maintenance of zebrafish and culture of embryos were carried out as described previously [32]. Embryos were staged by hours (hpf) or days (dpf) postfertilization at 28.5 °C.

1.2. Generation of transgenic zebrafish embryos with the deletion of ilf2 gene

Gene deletion was generated by introduction of indel into the *ilf2* gene via CRISPR/Cas9 and sgRNA procedure. The design and synthesis of sgRNA were carried out as described [33]. Briefly, CRISPRscan (http://www.crisprs-can.org/) was used to design sgRNA sequence against *ilf2*, and designs with high predicted efficiency and low predicted off-target effects were chosen. In brief, the forward and the reverse oligos were annealed and end-filled using Taq polymerase. Then the annealed end-filled DNA template was used to generate sgRNA specific for the target gene using MEGAshortscript T7 kit (Invitrogen) following manufacturer's protocol. DNA template was then removed by incubation with TURBO DNase at 37 °C for 15 min. 1 to 3 nl of injection mixture (sgRNA: 150 pg/nl; Cas9 protein: 667 pg/nl; 0.05% phenol red in RNase free water) was injected into the cytoplasm of one-cell stage um14Tg[Tg(tp1-MmHbb:EGFP)um14] embryos to generate knockout zebrafish larvae. The injected larvae and uninjected control were cultured to 5 dpf for phenotype checking and imaging.

Injected larvae were collected for genomic DNA extraction and T7E1 assay to confirm the presence of indel mutation as described previously [34]. In brief, the genomic region flanking the sgRNA target site was amplified by PCR. The PCR product was denatured and slowly reannealed to allow the formation of a heteroduplex. The reannealed PCR product was digested with T7 endonuclease I (New England Biolab) at 37 °C for 45 min and then resolved by 2% agarose gel electrophoresis. The sequence of sgRNA for *ilf2* is taatacgactcactataGGGGGCCGAGGTGGCCG GTTgttttagagctagaa. Primers for PCR amplification of *ilf2* for T7 endonuclease I analysis are: forward: 5′-GCTAGCTACTCGGCGGCTAT-3′; reverse: 5′-GCTCTGGGCTTAAAAAGGCTG-3′.

To confirm the successful knockout of *ilf2*, total RNA was extracted from 5-dpf embryos ($n = 5$) injected with the specific gRNA and Cas9 or with Cas9 (control) alone using RNeasy Mini Kit (Qiagen) and cDNA was reverse transcribed using PrimeScript RT reagent kit (RR047Q; TakaRa). PCR was performed using a Hot StarTaq (157011236; Qiagen). Expression of a house-keeping gene (*actb*) was included for comparison. PCR was performed in 25 μl of reaction mixture containing PCR buffer (Roche); MgCl2 (2.5 mM); dNTP (0.2 mM each); forward and reverse primers (0.1 nmol each); 3 μl DNA template and 2.5 U DNA polymerase (QIAGEN; HotStart Taq). The initial denaturation was performed at 95 °C for 5 min; PCR reaction was performed for 35 cycles described as follows: After initial 5 min denaturation at 95 °C; 30 s denaturation at 95 °C, 60 s annealing at specific temperature, 60 s extension at 72 °C for each cycle. An additional extension step was carried out for 10 min at 72 °C. PCR products were analyzed by electrophoresis in a 1.5% (*w*/*v*) agarose gel and stained by ethidium bromide which was visualized under UV illumination. Primers for RT-PCR analysis of *ilf2* mRNA are: forward: 5′-CAAGGGTATCGGCCCTTTGT-3′; reverse: 5′-ACAGCAGAGTGTCCCAACAG-3′. Primers for RT-PCR analysis of *actb* mRNA are: forward: 5′-CACACCGTGCCCATCTATGA-3′; reverse: 5′-AATGCGCCATACAGAGCAGA-3′.

1.3. Whole mount in-situ hybridization analysis

The DNA clone of *ilf2* was purchased from Source BioScience LifeSciences and subcloned into pBluescript vector for the generation of digoxigenin-labeled antisense and sense riboprobes. Whole-mount in situ hybridization was performed as described by Thisse et al. [35].

1.4. Whole mount fluorescence immunostaining

Zebrafish larvae were euthanized in ice water. After PBS wash, larvae were fixed in 4% PFA/PBS for at least 2 h, washed with PBS and then permeabilized with blocking buffer for 2 h in RT. Blocking buffer: 10% goat serum, 1% BSA, 1% DMSO in PBST. PBST: 0.2% Triton X-100 in PBS. Prepare diluted primary antibody in blocking buffer (200 μl per 10 embryos); prox-1 (1:100 dilution). Larvae were incubated for 2–3 days at 4 °C. After being washed with 10% blocking buffer in PBST (30 min each for 6 times), larvae were incubated with appropriate fluorescence conjugated secondary antibody (1:500 in blocking buffer) in dark at 4 °C overnight. Larvae were then washed with PBST (30 min each for 6 times) before being washed with PBS and finally in Milli-Q water. Larvae were then mounted in ProLong™ Gold Antifade Mountant (ThermoFisher Scientific) for imaging.

1.5. Section immunofluorescence analysis

Larvae (5-dpf) were fixed in PFA/PBS (4% (*w*/*v*) paraformaldehyde (Sigma-Aldrich, Steinheim, Germany) in PBS (phosphate-buffered saline, pH 7.2; Sigma-Aldrich, Steinheim, Germany) for 36 h at 4 °C, dehydrated in graded series of alcohol (Merck, Darmstadt, Germany),

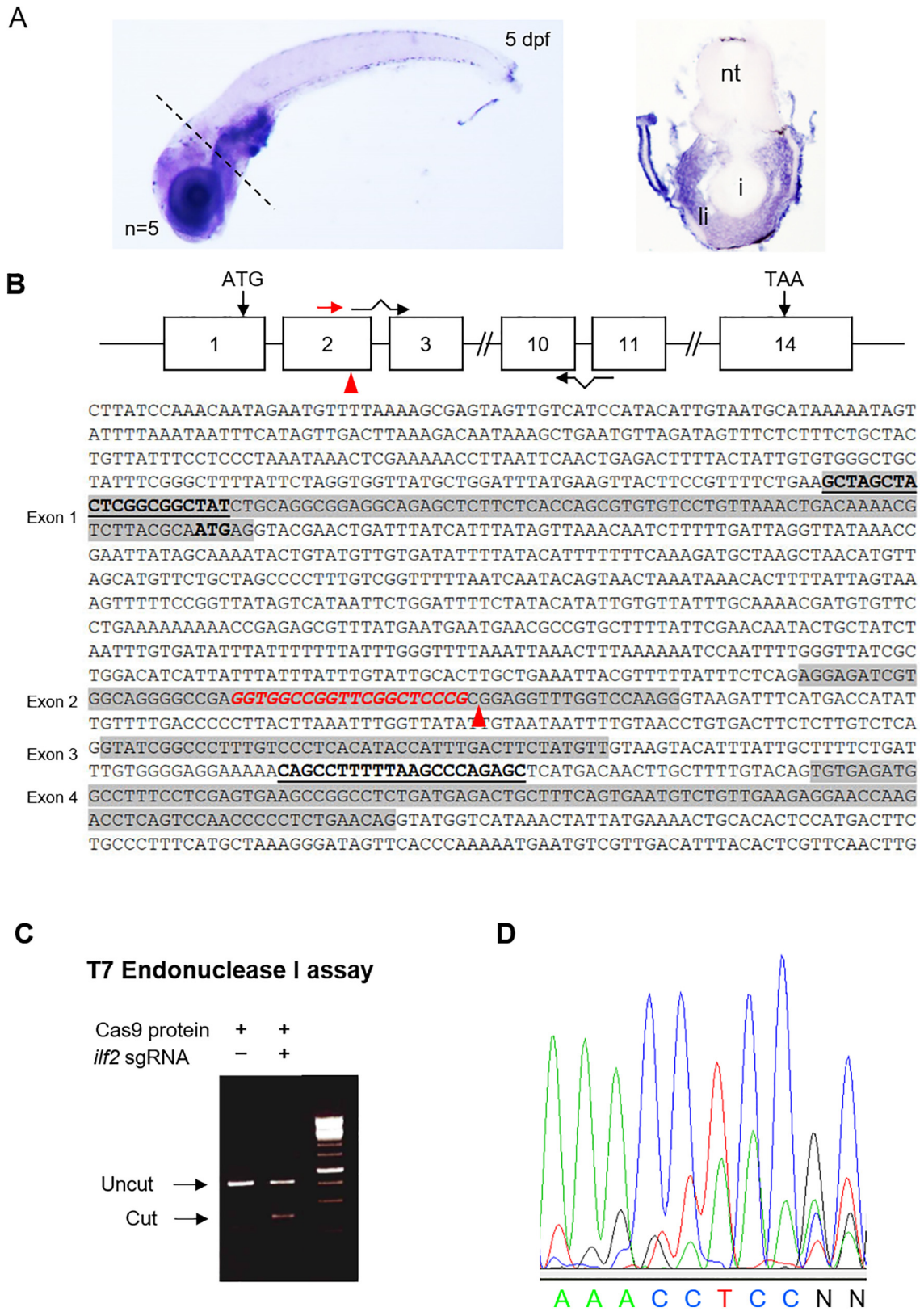

Fig. 1. Liver expression of *ilf2*. (A) Whole mount in situ hybridization (WISH) was performed on 5-dpf zebrafish larvae to detect the expression of the zebrafish homologs of human *ILF2* (blue). Transverse sectioning (dotted line) of WISH larvae was performed and shown on the left to confirm liver expression of BA candidate genes. (B) Structure of zebrafish *ilf2* gene and the sequence of the genomic region spanning exon 1 to exon 4 of the *ilf2* gene. The locations of the two exon-spanning primers for semiquantitation RT-PCR analysis of *ilf2* in control and *ilf2* knockout fish were shown as bended arrows. The sequence of the sgRNA targeted at the exon 2 was indicated in red. The primers for PCR amplification of the *ilf2* genomic region for T7 endonuclease I assay (C) and sequencing analysis (D) to confirm the successful indel introduction into the *ilf2* gene were highlighted in bold and underlined. C, Abbreviations: nt, neural tube; i, intestine; li, liver.

and cleared in xylene (RCI Labscan Ltd., Bangkok, Thailand) before being embedded in paraffin (Leica Biosystems, Richmond, IL USA). Transverse sections (6 μm in thickness) were prepared and mounted onto TESPA-coated microscope glass.

Sections were dewaxed in xylene and hydrated in a graded series of alcohol and finally in distilled water. Antigen retrieval was performed by incubation in 10 mM sodium citrate buffer (pH 6.0) at 95 °C for 10 min. After blocking in PBS-T (PBS with 0.1% Triton) supplemented with 1% bovine serum albumin (USB Corporation, Cleveland, OH USA) for 1 h at room temperature, sections were incubated with antizebrafish gut secretory cell epitopes ab [FIS 2F11/2] (Abcam ab71286; 1:100 dilution) in PBS-T overnight at 4 °C. The sections were washed in PBS-T before incubation with appropriate fluorochrome-conjugated secondary antibody (1:200, Invitrogen, Carlsbad, CA, USA) at 37 °C for 1 h. After washing with PBS-T, sections were mounted in mounting solution containing DAPI (Vectalabs, Burlingame, CA, USA).

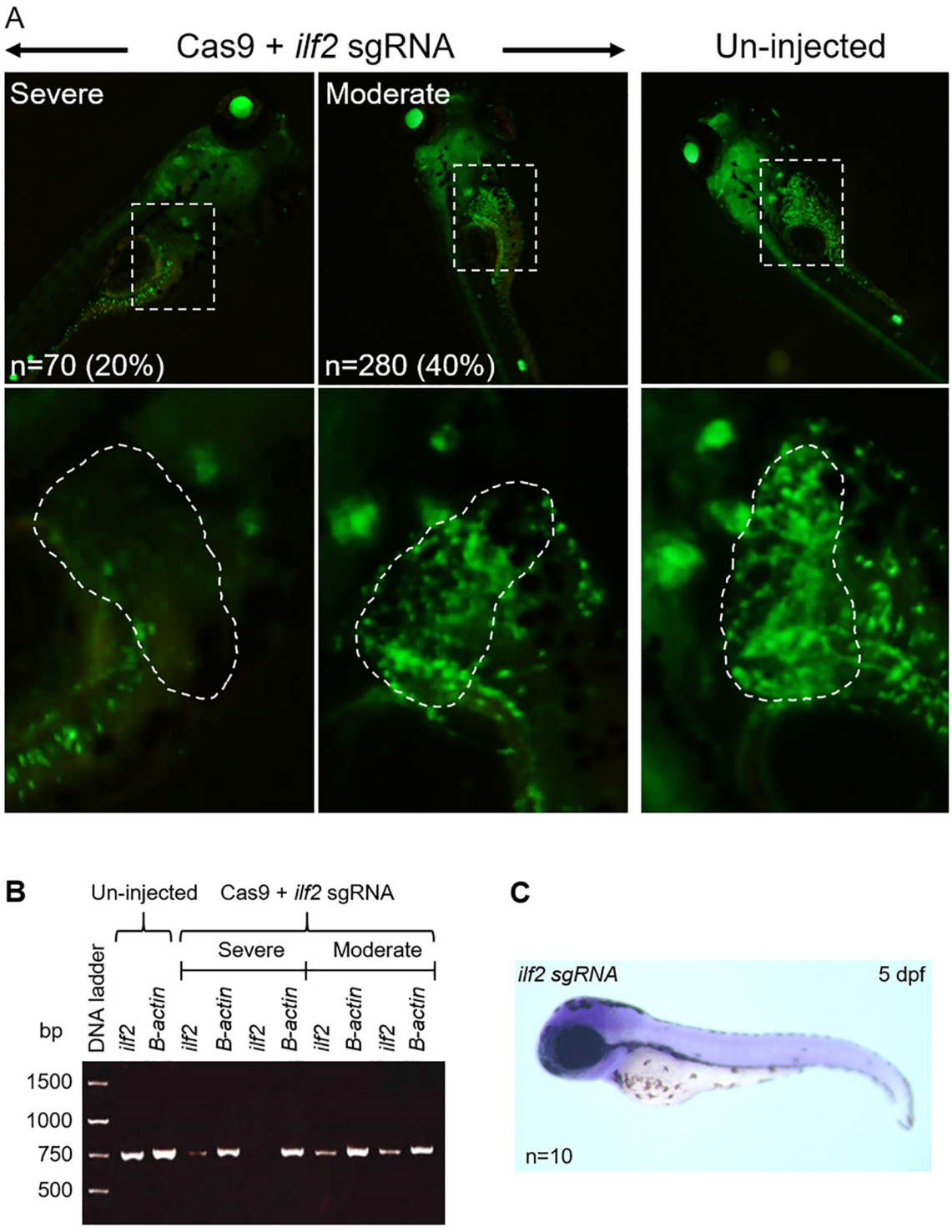

Fig. 2. Defective biliary development in *ilf2* mutant zebrafish. (A) 5-dpf *ilf2* mutant (Cas9 + *ilf2* sgRNA injected) and uninjected (Cas9 injected) larvae were examined under fluorescence microscope. Development of bile ducts (green) was severely and moderately defective in mutants. Regions highlighted in broken lines were magnified and shown below. Number of mutant and control larvae analyzed was indicated as "*n*". (B) Semiquantitative RT-PCR analysis of *ilf2* expression in uninjected, severe and moderate *ilf2* mutant larvae. Expression of beta-actin (B-actin) was used as internal control. (C) Whole mount in situ hybridization (WISH) was performed on 5-dpf *ilf2* mutant larvae (blue).

Percentages of 2F11 + ve biliary cells in livers of *Ilf2* sgRNA and uninjected 5 dpf larvae were determined by counting number of 2F11 + ve biliary cells and total liver cells on coronal sections. Percentages of 2F11 + ve biliary cells of the livers of *Ilf2* sgRNA and uninjected 5 dpf larvae were calculated by (2F11 + ve cells/DAPI + ve nuclei) × 100%. Ten embryos of each group were included for the analysis; six sections of liver of each larva were examined for the quantitation of the 2F11 + ve biliary cells. Percentages of apoptosis were shown as mean ± S.E.M.

1.6. Proliferation assay

Frozen sections (7 μm in thickness) of mutant and control 5 dpf larvae were prepared and processed for immunofluorescence staining following standard protocol. Sections were costained with anti-PCNA antibody (ab29; abcam; 1:500 dilution) and 2F11/2 (Abcam ab71286; 1:100 dilution) in PBS-T overnight at 4 °C. The sections were washed in PBS-T before incubation with appropriate fluorochrome-conjugated secondary antibody (1:200, Invitrogen, Carlsbad, CA, USA) at 37 °C for 1 h. After washing with PBS-T, sections were mounted in mounting solution containing DAPI (Vectalabs, Burlingame, CA, USA).

1.7. TUNEL assay

Apoptotic cells on sections were detected using In Situ Cell Death Detection Kit following manufacturer's protocol (Roche Applied Science, Indianapolis, IN, USA). Images were taken with Nikon Eclipse 80i microscope (Melville, NY, USA) mounted with SPOT RT3 microscope digital camera (DIAGNOSTIC Instruments, Inc., Sterling Heights, MI, USA) under fluorescence illumination for the DAPI + ve nuclei and TUNEL + ve cells. Photos were compiled using Adobe Photoshop 7.

1.8. Statistical analysis

Student's t test was performed to calculate the differences between groups, and *p* value less than 0.05 was regarded as statistically significant.

2. Results

2.1. ILF2 was expressed in the developing liver of zebrafish larvae

To investigate if *ILF2* was expressed in zebrafish larvae, whole mount in situ hybridization (WISH) was performed on 5-dpf zebrafish larvae. Expression of the zebrafish homologs of human *ILF2* (*ilf2*) was detected in the developing liver of 5-dpf zebrafish larvae; sectioning of the WISH larvae further confirmed the liver expression of *ilf2* (Fig. 1A).

2.2. Knockout of ilf2 caused defective biliary development

Using CRISPR/Cas9 gene knockout approach and sgRNA targeting the exon 2 of *ilf2* gene in the transgenic fish line (um14Tg[Tg(tp1-MmHbb:EGFP)um14], we generated zebrafish larvae carrying indel at *ilf2* (Fig. 1B). Genomic DNAs were extracted from uninjected (Cas9 protein alone) and *ilf2* sgRNA injected (Cas9 protein + *ilf2* sgRNA) 5-dpf larvae for PCR amplification using primers (bold and underlined; Fig. 1B) flanking the exon 1 and the intron 3 of the *ilf2* gene. T7 endonuclease I assay (Fig. 1C) and sequencing analysis using the intron 3 primer (Fig. 1D) confirmed a successful introduction of indel at the exon 2 of the *ilf2* gene (red arrowhead; Fig. 1B) and a truncation mutation.

The biliary development of uninjected (Cas9 protein alone) and *ilf2* sgRNA injected (Cas9 protein + *ilf2* sgRNA) 5-dpf larvae was studied by examining the bile duct green fluorescence signal intensity under

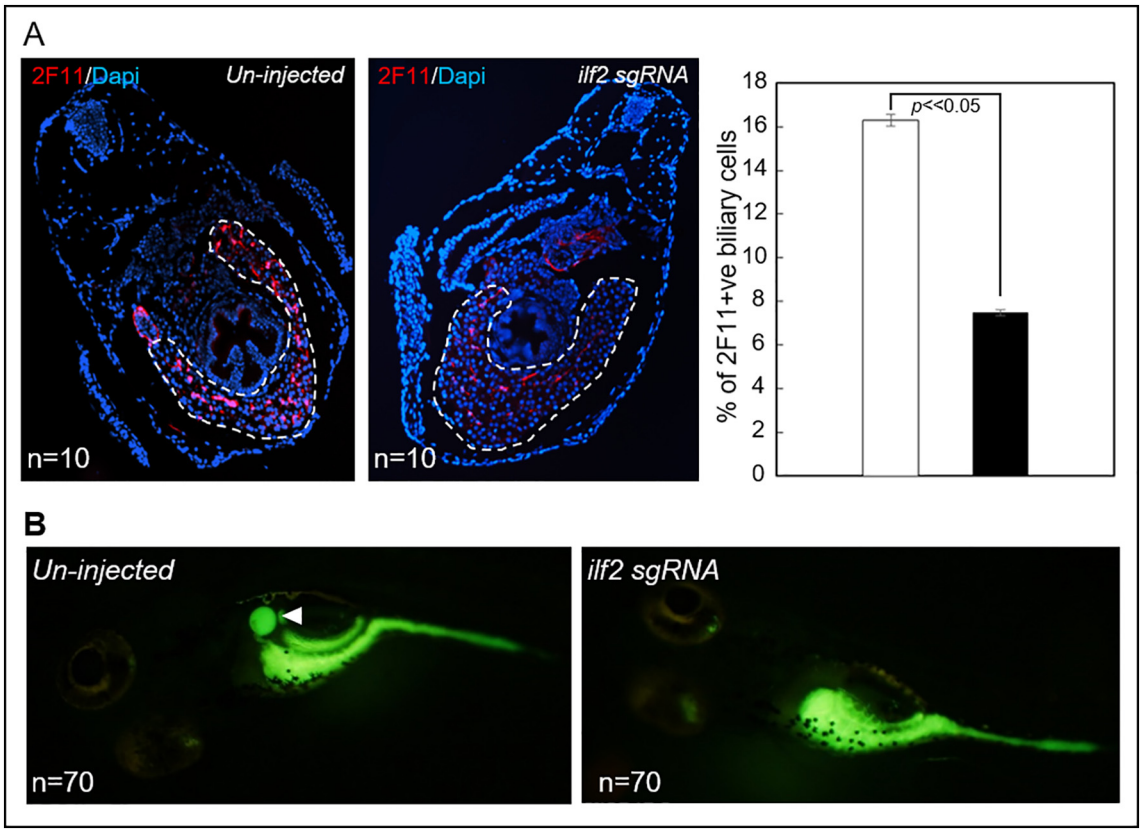

Fig. 3. Reduced number of bile duct cells and absence of bile flow in *ilf2* mutant zebrafish. (A) Bile ducts of mutant and control larvae were examined and quantified by section immunostaining for 2F-11 (bile duct marker). Number of bile duct cells (red) was significantly reduced in mutant liver (B). Livers were highlighted with broken lines. (B) Bile flow from liver to gall bladder (arrowhead) of mutants and controls was examined with PED6 assay. Absence of gall bladder fluorescence in mutant larvae indicated an absence of bile flow from liver to gall bladder. Number of mutant and control larvae analyzed was indicated as "*n*".

fluorescence microscope. Zebrafish larvae with the knockout of *ilf2* showed severe to moderate reduction of biliary green fluorescence signal as compared to control larvae (Fig. 2A). RT-PCR analysis (Fig. 2B) and WISH assay (Fig. 2C; compared to Fig. 1A) confirmed a knockout of *ilf2* resulted in marked reduction of its mRNAs. The degree of the reduction of *ilf2* expression in mutant larvae correlated with the severity of biliary development defect, in that mutant larvae with severe biliary defect displayed a greater reduction of *ilf2* expression than that in mutant larvae with moderate biliary defect (Fig. 2B).

To further confirm the defective biliary development in *ilf2* knockout larvae, sections of mutant and control larvae were immunostained for bile duct marker 2F-11. A significant reduction of 2F-11 immunoreactive bile duct cells was observed in *ilf2* knockout larvae (Fig. 3A). In line with the defective biliary development in *ilf2* mutant larvae, PED6 fluorescence was absent in the gall bladder, whereas the control embryos showed strong PED6 fluorescence in the gall bladder (Fig. 3B).

To determine if defective biliary development of *ilf2* mutants was attributed to apoptosis and/or defective proliferation of bile duct cells, we performed TUNEL and immunostaining for proliferative marker PCNA. TUNEL positive cells were rarely found in mutant and control livers (Fig. 4A). PCNA and GFP double positive proliferating bile duct cells in the mutant and control livers were comparable (Fig. 4B).

To investigate the differentiation of liver progenitors (hepatoblasts) in *ilf2* mutant and control larvae, whole-mount immunostaining for hepatoblasts marker prox-1 was performed on 3-dpf mutant and control larvae. Reduced immunoreactivity of prox-1 was detected within the hepatic anlage of mutant larvae as compared to that of control larvae at 3-dpf (Fig. 5), suggesting that differentiation of hepatoblasts was delayed in *ilf2* mutant larvae.

3. Discussion

Genomic rearrangements leading to the appearance of copy number variations (CNVs) play an important role in human disease. We identified 28 BA-unique CNV regions (>100 kb each) that interfered with a total of 102 genes (76 duplicated and 26 deleted). These BA-CNVs

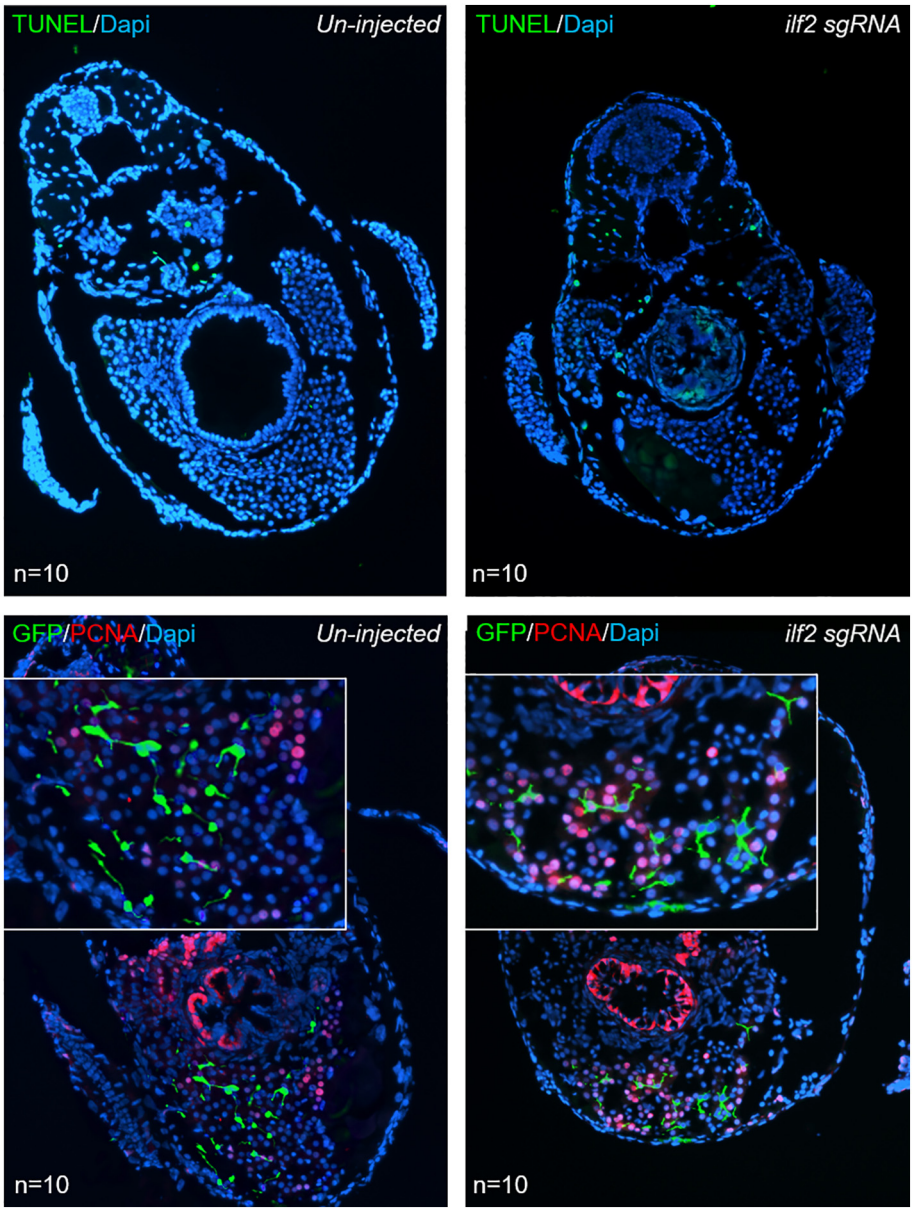

Fig. 4. Knockout of *ilf2* did not induce apoptosis and defective proliferation of bile duct cells. (A) Apoptosis of 5-dpf mutant and control larvae was examined by TUNEL assay. (B) Proliferative biliary cells of 5-dpf mutant and control larvae were identified by immunofluorescence staining for PCNA (red) and GFP fluorescence (green). Livers were highlighted with broken lines. Number of mutant and control larvae analyzed was indicated as "*n*".

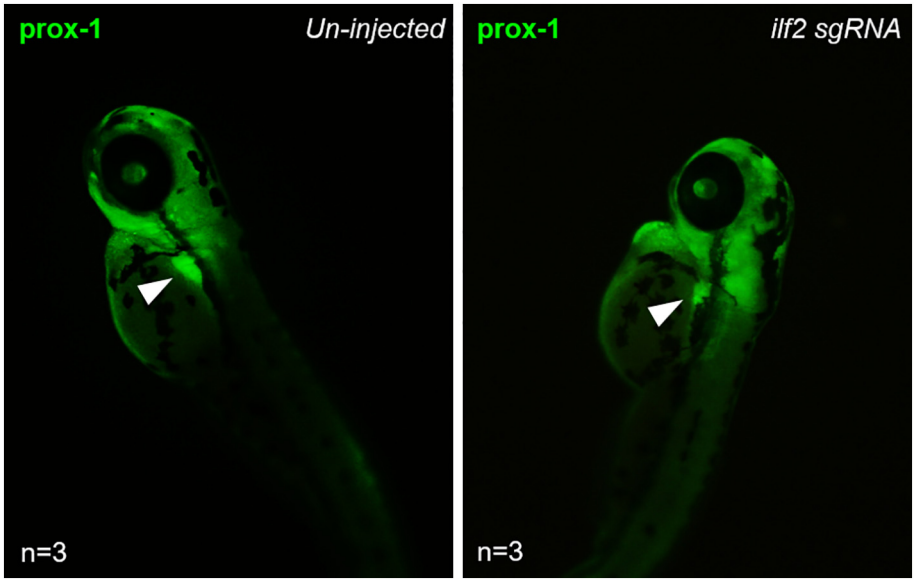

Fig. 5. Development of hepatic anlage and hepatoblasts was unaffected by *ilf2* knockout. 3-dpf mutant and control larvae were examined by whole mount immunostaining for prox-1 (green; arrowheads) to investigate the development of hepatic anlage and hepatoblasts. Number of mutant and control larvae analyzed was indicated as "*n*".

biologically converged into immune pathway, suggesting that genes relevant in immune regulation within BA-CNVs likely contributed to BA [12]. We selected the *ILF2* (deleted in a BA-CNV) according to its human liver expression in [27] and its functions in the differentiation of stem cells [24–26] for functional evaluation by CRISPR/Cas9 gene knockout approach to study its impacts in biliary development. We showed that CRISPR/Cas9 knockout of *ILF2* (interleukin enhancer binding factor 2, involved in innate immune regulation) caused a defective biliary development in zebrafish.

In *ilf2* mutant larvae, the bile duct was underdeveloped, resulting in a sparse biliary network resembling a biliary ductopenia, which has been reported in the liver of BA patients. Hepatoblasts are bipotential liver stem cells and give rise to bile duct cells (cholangiocytes) and liver cells (hepatocytes) in embryonic hepatobiliary development and in liver regeneration/repair [36]. Differentiation of liver progenitor cells (hepatoblasts; prox-1 immunopositive) appeared affected by the deletion of *ilf2* in mutant, suggesting that *ilf2* function may be crucial for the development of the hepatic anlage and hepatoblasts. However, deletion of *ilf2* did not induce apoptosis and did not affect the proliferation of bile duct cells, indicating that *ilf2* is not essential for the survival and the proliferation of bile duct cells. Taking all the above suggested that *ilf2* function is likely involved in the differentiation of hepatoblasts, in that deletion of *ilf2* leads to a defective hepatobiliary differentiation resulting in an abnormally sparse biliary network. In line with the abnormal biliary network of *ilf2* mutant, a reduced liver to gall bladder bile flow as revealed by the absence of PED6 fluorescence in mutant gall bladder was observed. Taken all these indicated that deletion of *ilf2* caused a reduced bile flow and defect in the biliary structure — a phenocopy of BA in human.

ILF2 gene was first identified to be required for interleukin 2 expression in T-cell [13–15]. ILF2 also play an essential role in the encapsidation and protein priming of hepatitis B viral polymerase [37]. Later, ILF2 was shown to be involved in diverse cellular processes and functions in many different cell types such as cytoplasmic distribution and stability [16,17], processing and translation [18–20] of mRNA, DNA breaks repair [21,22], and microRNA processing [23]. Furthermore, ILF2 also regulates cell cycle exit and myogenic differentiation [24,25], pluripotency and differentiation of embryonic stem cells [26]. Knockdown of ILF2 or ILF3 protein retards cell growth, possibly by inhibition of a diverse posttranscriptional processing of mRNA. *ILF2* is expressed in multiple tissues of human and mouse including liver [27]. Transcripts of *ILF2* homolog *ilf2* could also be detected in the early developing liver of zebrafish larvae, suggesting that *ilf2* may also be involved in the early hepatobiliary development. Indeed, a deletion of *ilf2* in zebrafish embryos delays the development of the hepatic anlage and hepatoblasts, leading to a defective biliary tree development as seen in this study.

In summary, deletion of *ilf2* caused a reduced bile flow and defect in the biliary structure — a phenocopy of BA in human. It is worthwhile in the future (i) to study the embryonic biliary development and (ii) to compare BA development/progress as induced by virus (RRV) or toxins (biliatresone) in heterozygous/homozygous *ilf2* knockout and wild-type mice to further clarify the roles of *ILF2* in embryonic biliary development and in BA pathogenesis. In addition, our study showed that CRISPR/Cas9 gene knockout of genes interfered by BA-CNVs in zebrafish is an efficient platform to functionally evaluate BA candidate genes in biliary development and in the pathogenesis of BA.

Acknowledgments

This work is supported by the Health and Medical Research Fund (Project No.: 03141296), Hong Kong Special Administrative Region Government to V.C.H.L.

Authors' contributions

Study concept and design: V.C.H.L., and A.C.H.M. Data acquisition: Y.C., Z.W. and V.C.H.L. Analysis and interpretation of the data: V.C.H.L., M/.M.G.B., P.K.H.T. and A.C.H.M. Drafting of the manuscript: Y.C. and V.C.H.L.

Ethics approval

All the animal experiment protocols were approved by the Committee on the Use of Live Animals in Teaching & Research, The University of Hong Kong (CULATR No.: 3745-15).

Declaration of competing interests

Authors declare no competing interests.

Availability of data and materials

The datasets used and/or analyzed during the current study are available from the corresponding author on reasonable request.

References

[1] Tam PKH, Yiu RS, Lendahl U, et al. Cholangiopathies — towards a molecular understanding. EBioMedicine. 2018;35:381–93.
[2] Sanchez-Valle A, Kassira N, Varela VC, et al. Biliary atresia: epidemiology, genetics, clinical update, and public health perspective. Adv Pediatr. 2017;64(1):285–305.
[3] Hartley JL, Davenport M, Kelly DA. Biliary atresia. Lancet. 2009;374(9702):1704–13.
[4] Tam PKH, Chung PHY, St Peter SD, et al. Advances in paediatric gastroenterology. Lancet. 2017;390(10099):1072–82.
[5] Chung PH, Wong KK, Tam PK. Predictors for failure after Kasai operation. J Pediatr Surg. 2015;50(2):293–6.
[6] Ernest van Heurn LW, Saing H, Tam PK. Cholangitis after hepatic portoenterostomy for biliary atresia: a multivariate analysis of risk factors. J Pediatr. 2003;142(5):566–71.
[7] Khong PL, Ooi CG, Saing H, et al. Portal venous velocity in the follow-up of patients with biliary atresia after Kasai portoenterostomy. J Pediatr Surg. 2002;37(6):873–6.
[8] Wong KK, Fan AH, Lan LC, et al. Effective antibiotic regime for postoperative acute cholangitis in biliary atresia—an evolving scene. J Pediatr Surg. 2004;39(12):1800–2.
[9] Mysore KR, Shneider BL, Harpavat S. Biliary atresia as a disease starting in utero: implications for treatment, diagnosis, and pathogenesis. J Pediatr Gastroenterol Nutr. 2019;69(4):396–403.
[10] Cheng G, Tang CS, Wong EH, et al. Common genetic variants regulating ADD3 gene expression alter biliary atresia risk. J Hepatol. 2013;59(6):1285–91.
[11] Garcia-Barcelo MM, Yeung MY, Miao XP, et al. Genome-wide association study identifies a susceptibility locus for biliary atresia on 10q24.2. Hum Mol Genet. 2010;19(14):2917–25.
[12] Cheng G, Chung PH, Chan EK, et al. Patient complexity and genotype-phenotype correlations in biliary atresia: a cross-sectional analysis. BMC Med Genomics. 2017;10(1):22.
[13] Shaw JP, Utz PJ, Durand DB, et al. Identification of a putative regulator of early T cell activation genes. Science. 1988;241(4862):202–5.
[14] Kao PN, Chen L, Brock G, et al. Cloning and expression of cyclosporin A- and FK506-sensitive nuclear factor of activated T-cells: NF45 and NF90. J Biol Chem. 1994;269(32):20691–9.
[15] Corthesy B, Kao PN. Purification by DNA affinity chromatography of two polypeptides that contact the NF-AT DNA binding site in the interleukin 2 promoter. J Biol Chem. 1994;269(32):20682–90.
[16] Shim J, Lim H, J RY, et al. Nuclear export of NF90 is required for interleukin-2 mRNA stabilization. Mol Cell. 2002;10(6):1331–44.
[17] Barber GN. The NFAR's (nuclear factors associated with dsRNA): evolutionarily conserved members of the dsRNA binding protein family. RNA Biol. 2009;6(1):35–9.
[18] Merrill MK, Gromeier M. The double-stranded RNA binding protein 76:NF45 heterodimer inhibits translation initiation at the rhinovirus type 2 internal ribosome entry site. J Virol. 2006;80(14):6936–42.
[19] Kuwano Y, Pullmann Jr R, Marasa BS, et al. NF90 selectively represses the translation of target mRNAs bearing an AU-rich signature motif. Nucleic Acids Res. 2010;38(1):225–38.
[20] Graber TE, Baird SD, Kao PN, et al. NF45 functions as an IRES trans-acting factor that is required for translation of cIAP1 during the unfolded protein response. Cell Death Differ. 2010;17(4):719–29.
[21] Shamanna RA, Hoque M, Lewis-Antes A, et al. The NF90/NF45 complex participates in DNA break repair via nonhomologous end joining. Mol Cell Biol. 2011;31(23):4832–43.
[22] Marchesini M, Ogoti Y, Fiorini E, et al. ILF2 is a regulator of RNA splicing and DNA damage response in 1q21-amplified multiple myeloma. Cancer Cell. 2017;32(1):88–100 [e6].
[23] Sakamoto S, Aoki K, Higuchi T, et al. The NF90-NF45 complex functions as a negative regulator in the microRNA processing pathway. Mol Cell Biol. 2009;29(13):3754–69.
[24] Todaka H, Higuchi T, Yagyu K, et al. Overexpression of NF90-NF45 represses myogenic microRNA biogenesis, resulting in development of skeletal muscle atrophy and centronuclear muscle fibers. Mol Cell Biol. 2015;35(13):2295–308.
[25] Shi L, Zhao G, Qiu D, et al. NF90 regulates cell cycle exit and terminal myogenic differentiation by direct binding to the 3′-untranslated region of MyoD and p21WAF1/CIP1 mRNAs. J Biol Chem. 2005;280(19):18981–9.
[26] Ye J, Jin H, Pankov A, et al. NF45 and NF90/NF110 coordinately regulate ESC pluripotency and differentiation. RNA. 2017;23(8):1270–84.
[27] Zhao G, Shi L, Qiu D, et al. NF45/ILF2 tissue expression, promoter analysis, and interleukin-2 transactivating function. Exp Cell Res. 2005;305(2):312–23.
[28] Cheung ID, Bagnat M, Ma TP, et al. Regulation of intrahepatic biliary duct morphogenesis by Claudin 15-like b. Dev Biol. 2012;361(1):68–78.
[29] Garnaas MK, Cutting CC, Meyers A, et al. Rargb regulates organ laterality in a zebrafish model of right atrial isomerism. Dev Biol. 2012;372(2):178–89.
[30] Schaub M, Nussbaum J, Verkade H, et al. Mutation of zebrafish Snapc4 is associated with loss of the intrahepatic biliary network. Dev Biol. 2012;363(1):128–37.
[31] Wilkins BJ, Gong W, Pack M. A novel keratin18 promoter that drives reporter gene expression in the intrahepatic and extrahepatic biliary system allows isolation of cell-type specific transcripts from zebrafish liver. Gene Expr Patterns. 2014;14(2):62–8.
[32] Westerfield M. The zebrafish book. A guide for the laboratory use of zebrafish (Danio rerio). 4th ed.. University of Oregon Press, Eugene; 2000.
[33] Moreno-Mateos MA, Vejnar CE, Beaudoin JD, et al. CRISPRscan: designing highly efficient sgRNAs for CRISPR-Cas9 targeting in vivo. Nat Methods. 2015;12(10):982–8.
[34] Jao LE, Wente SR, Chen W. Efficient multiplex biallelic zebrafish genome editing using a CRISPR nuclease system. Proc Natl Acad Sci U S A. 2013;110(34):13904–9.
[35] Thisse C, Thisse B, Schilling TF, et al. Structure of the zebrafish snail1 gene and its expression in wild-type, spadetail and no tail mutant embryos. Development. 1993;119(4):1203–15.
[36] Lemaigre FP. Development of the biliary tract. Mech Dev. 2003;120(1):81–7.
[37] Shin HJ, Kim SS, Cho YH, et al. Host cell proteins binding to the encapsidation signal epsilon in hepatitis B virus RNA. Arch Virol. 2002;147(3):471–91.